

THE EVALUATION OF CEMENTATION
MECHANISMS IN KAOLINITE

A THESIS

Presented to

The Faculty of the Division of Graduate
Studies and Research

By

Lyndall Charles Webb

In Partial Fulfillment
of the Requirements for the Degree
Master of Science in Geophysical Sciences

Georgia Institute of Technology

August, 1974

THE EVALUATION OF CEMENTATION
MECHANISMS IN KAOLINITE

Approved:

C. E. Weaver, Chairman

C. O. Pollard

Randall Hughes

Date approved by Chairman:

8-20-74

ACKNOWLEDGMENTS

Sincere appreciation is expressed to Dr. C. E. Weaver for his counsel, assistance, encouragement, and especially for the use of his unique idea.

Gratitude is expressed to the Thiele Kaolin Company for providing the financial assistance and the background information necessary for the successful evaluation of the topic.

I also wish to thank Dr. C. O. Pollard and Dr. Randall Hughes for providing critical thesis reviews.

TABLE OF CONTENTS

	Page
ACKNOWLEDGMENTS	ii
LIST OF TABLES	iv
LIST OF ILLUSTRATIONS	v
SUMMARY	vi
Chapter	
I. INTRODUCTION	1
II. ANALYSIS OF CRUDE KAOLINITE	6
Instrumentation and Techniques Characterization	
III. ALUMINUM TREATED KAOLINITE	20
Treatment Results and Discussion	
IV. CONCLUSIONS	39
BIBLIOGRAPHY	40

LIST OF TABLES

Table	Page
1. Proposed Development of Aluminum Hydroxide	3
2. Crystallinity Index Values for KS	14
3. Cation Exchange Capacities--KS	14
4. Effect of Particle Size on Dehydroxylation Peak Area T _{max} , T _{start} , and T _{end}	17
5. Changes in Cementation Resulting from Aluminum Exchange Prior to Treatment with AlCl ₃	22
6. Alterations in Cementation with Increasing Weight Percent Chemicals Added	23
7. Concentrations of AlCl ₃ Used to Evaluate Cementation	27

LIST OF ILLUSTRATIONS

Figure	Page
1. Method for Calculating Centrifuge Sedimentation Intervals	7
2. Computation of Crystallinity Index	7
3. Diffraction Patterns for KS	13
4a. S.E.M. Micrographs Illustrating Typical Fine-Grained Texture of KS	15
4b. Relatively Rare Large Kaolinite Books Found in KS	15
5. Effect of Amorphous Si-Al on Illite XRD Peak Intensity . . .	17
6. Particle Size Distribution for KB, KS	19
7. Effect of OH/Al Ratio on Cementation	22
8. Cementation Over a Range of OH/Al Ratios From 0.005-1.5 . . .	23
9. Range of Cementation Using 1 Gram KS and AlCl_3	26
10. The Effect of pH on Cementation	27
11. The Effect of Treatment Solution Concentration on Cementation	29
12. Cementation as a Function of Drying Temperature	29
13. Particle Size Alteration of Untreated Standards Over a Range of Drying Temperatures	31
14. Particle Size Distribution for Treated and Untreated KS . . .	31
15. The Distribution of Aluminum Species in Aqueous Solution . .	33
16. The Abundance of Complexed and Free Al^{+3} Related to Cementation	33
17. Stereo T.E.M. Micrographs Revealing Morphology of Cemented Kaolinite	38
18. S.E.M., T.E.M. Micrographs of Cemented Kaolinite Particles (Rounded Edges are Due to Attempted Blender Dispersion) . . .	39

SUMMARY

Solutions of aluminum in varying concentrations were used to alter the particle-size distribution of a kaolinite and produce a coarser product. The kaolinite sample, obtained from the Thiele Kaolin Company at Wrens, Georgia, is noted for its unusually fine-grained texture. The character of the clay was evaluated using x-ray powder diffraction, scanning and transmission electron microscopy, atomic absorption spectrophotometry, differential thermal analysis and centrifugation. A size analysis of the kaolinite indicates a large percentage of the sample is included in the size range 1-0 microns. Treated samples were examined to determine the percentage finer than 0.5 microns. Percentages obtained were compared to an untreated counterpart and also to a kaolinite sample possessing a typical size distribution. The evaluation of treated samples at 0.5 microns provides a gauge for treatment efficiency.

The kaolinite was treated with solutions of AlCl_3 , $\text{Al}(\text{NO}_3)_3$, and $\text{Al}_2(\text{SO}_4)_3$ and dried at temperatures ranging from 50-300°C. Drastic reductions in the percentage finer than 0.5 microns were noted using AlCl_3 and, to some extent, $\text{Al}(\text{NO}_3)_3$.

The primary factor in the cementation mechanism seems to be an increased concentration of Al^{+3} ions prior to drying. During drying, kaolinite particles apparently aggregate about highly charged aluminum polymers created as a result of increased temperature. The polymerization of aluminum increases with temperature (Rich 1960).

Aggregates produced were stable enough to withstand attempted

dispersion using sodium polyphosphate and a high-speed 250 ml blender.

Aluminum sulfate was inefficient at producing aggregates other than floccules. Floccules are defined here to be reversible combinations of clay flakes. The formation of extremely stable aluminum hydroxy-sulfates is thought to be responsible for the lack of cementation using aluminum sulfate. Complexes of aluminum sulfate would effectively reduce the amount of Al^{+3} available for interaction with the clay.

Examination of cemented particles using electron microscopy reveals aggregates which are constructed by the accumulation of small flakes onto the surface of larger particles. The small flakes appear to be concentrated on the basal surfaces; however, a few were noted adhering to edge sites. Nondispersive x-ray analyses in the scanning electron microscope demonstrate that in fact the large aggregates have higher Al-Si ratios than typical non-treated kaolinite.

CHAPTER I

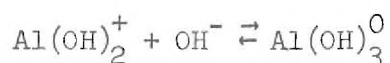
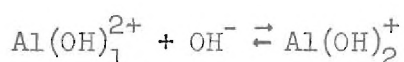
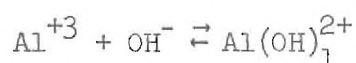
INTRODUCTION

Kaolinite is widely utilized as a coating material for paper products. Reading print, as well as writing paper, employs kaolinite as a surface coating. The kaolinite functions to increase sheet opacity. Fine-grained kaolinite, when used for this purpose, imparts a gloss to the paper which makes reading and even viewing difficult. If a process could be established which would effectively alter the particle size distribution of a fine-grained kaolinite, paper coated with this product would exhibit higher brightness and lower gloss. Brightness is a measure of light scatter whereas gloss refers to an absence of scatter. Paper coated with a relatively coarse-grained kaolinite displays a glare-free surface. The low glare results primarily from a lack of preferred orientation. A more random coating orientation also increases random light scatter which in effect improves brightness.

In order for a process of this type to effectively cement kaolinite flakes, it must employ bonds strong enough to withstand agitation and attempted chemical dispersion.

Aluminum in solution readily combines with OH^- to form hydroxy-aluminum complexes (Hsu, Bates 1964 and Jackson 1963). The size of the complexes is variable and depends solely upon pH and available OH^- . In solutions of relative OH^- depletion, these complexes exhibit an overall positive charge. The charge originates from a lack of charge

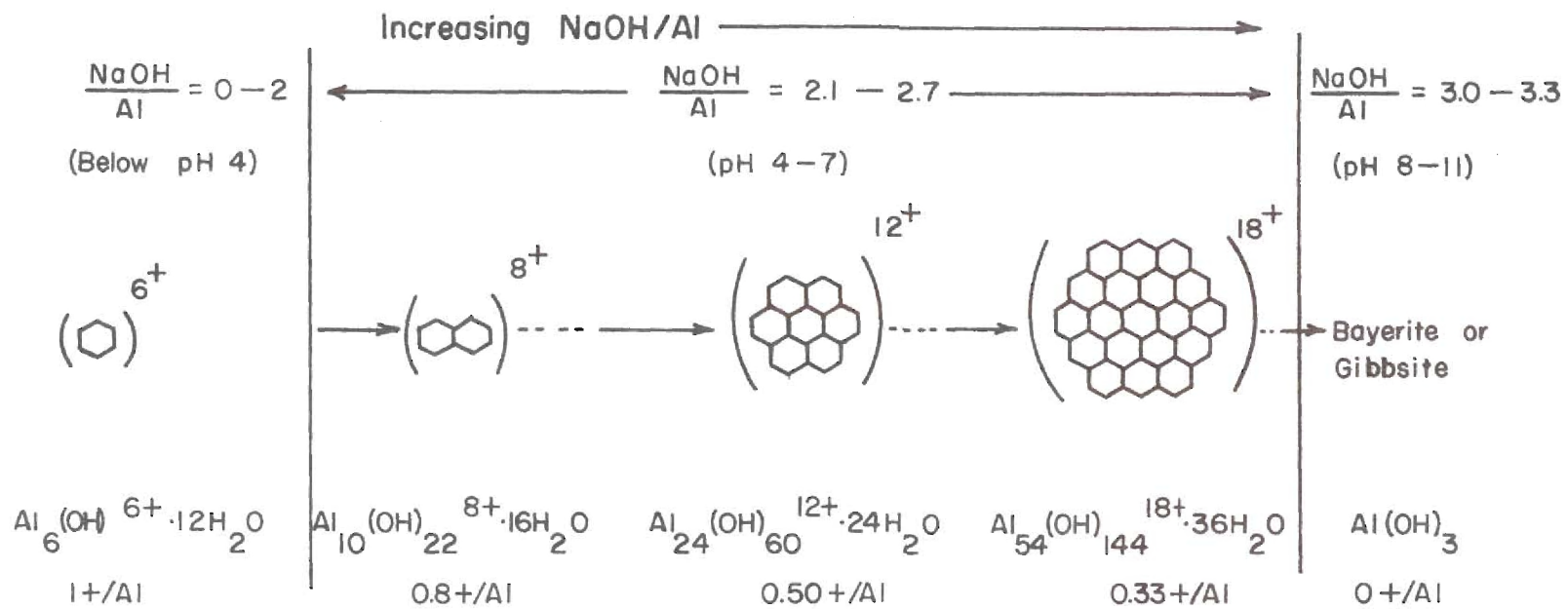
balance within the complex. The magnitude of the charge is also dependent upon pH. The smaller, more highly charged, species are present at low pH values. Over the pH range 3-7, the complexes vary in composition and charge from $\text{Al}(\text{OH})_1^{+2} \rightarrow \text{Al}(\text{OH})_3^0$. Near pH 7 a solid phase is formed. The stepwise formation of these complexes can be summarized by simple hydrolysis reactions:



Hsu and Bates (1964) have extensively investigated the formation of amorphous and crystalline aluminum hydroxides. Their findings indicate that it is possible to predict the aluminum species present in solution at any given time if the OH-Al ratio is predetermined. Table 1 summarizes information obtained through their investigation of aluminum complexes.

Clay minerals, like aluminum complexes, may exhibit a charge imbalance. In most clays, however, the static charge is negative and originates from isomorphous substitution within the clay structure. Kaolinite possesses a charge deficiency which is the result of broken edge bonds. In solutions of aluminum, negatively charged clay minerals display an attractive force for the oppositely charged aluminum complexes. In this manner, clay minerals may acquire a coating of amorphous aluminum hydroxide. Hydroxides of iron and magnesium may also be adsorbed in this manner. E. A. C. Follett (1965) described the sorption of ferric hydroxide on the surfaces of kaolinite flakes.

Table 1. Proposed Development of Aluminum Hydroxide



(After Hsu and Bates, 1964)

His observations suggest that the kaolinite-colloid complex, once produced, is extremely stable and not affected by changes in pH, ultrasonic vibrations, or repeated water washings. Studies by Follett and others have identified the basal surfaces as the actual sites of adsorption. Jenny and Smith (1935) reported the formation of alternating layers of iron hydroxide and kaolinite in pan formations. Pan formations are the accumulation of colloidal clay particles in the B-horizon of the soil profile. Their experiments on mutual flocculation indicated that pan formations may occur in the absence of electrolyte, providing positive colloids are present.

Hsu and Bates (1964), C. I. Rich (1959), and R. C. Turner (1967) have investigated the complicated interaction between hydroxides of aluminum and various clay minerals. All have recognized certain basic characteristic interactions:

- (1) aluminum is removed from solution by clay minerals
- (2) cation exchange capacities are drastically reduced in the presence of aluminum complexes
- (3) aluminum complexes, once adsorbed, are difficult to remove
- (4) aluminum migrates to interlayer positions in the expandable clays
- (5) expandable clay minerals lose a portion of their capacity to swell when saturated with hydroxy aluminum solutions.

The characteristics listed above suggest a chemically powerful and complex interaction.

The research described herein is an attempt to evaluate these

possibilities and examine the feasibility of cementing kaolinite with aluminum hydroxide.

CHAPTER II

ANALYSIS OF CRUDE KAOLINITE

Instrumentation and Techniques

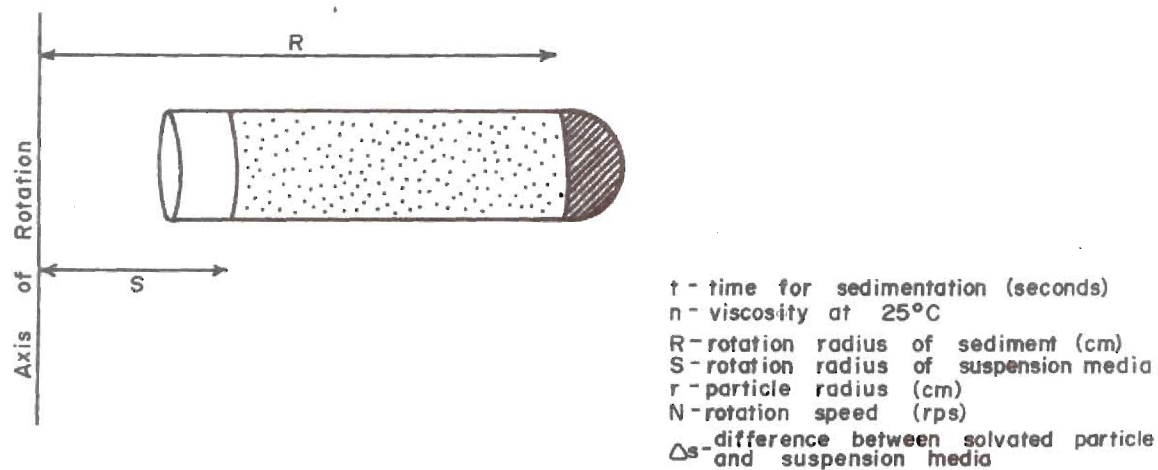
The kaolinite to be evaluated (designated KS) was collected at the Thiele Kaolin Company near Wrens, Georgia, in June 1973. It was sealed in glass containers and stored in a refrigerated area to reduce natural water loss. Pre-treatment analyses which could be affected by water loss were initiated as soon as practical.

Size Analysis

One hundred grams of KS were dispersed in a Waring blender with the aid of 1.0 gram of sodium polyphosphate. Blender agitation was continued for five minutes. The particle size distribution was then examined using an International Centrifuge Model UV and a centrifuge-pipette method. Ten milliliters of the dispersed-bulk sample were withdrawn by pipette and dried at 110°C. The aliquot was weighed. The weight recorded represented the weight of KS in 10 mls bulk sample. The clay suspension was centrifuged for prescribed time intervals calculated using an integrated form of Stokes Law:

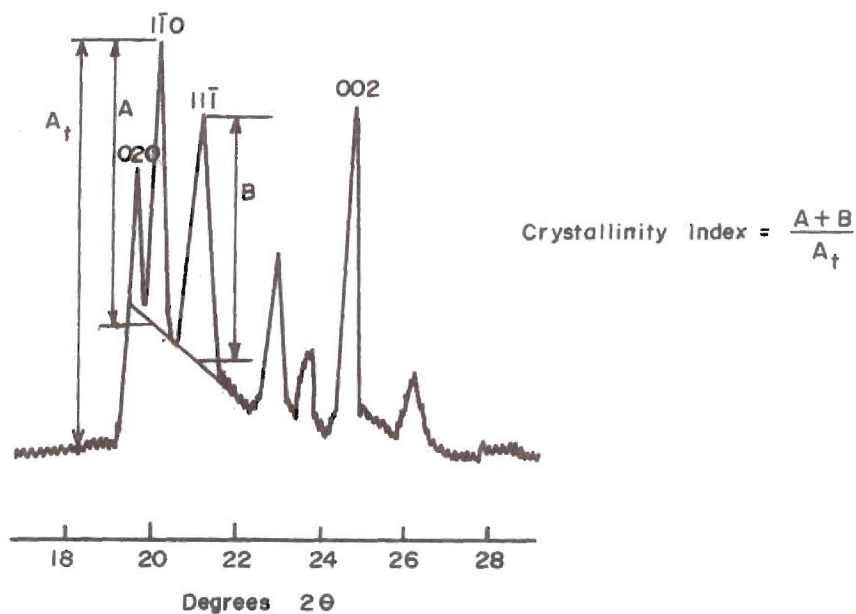
$$t = \frac{n \log_{10} R/S}{3.81 N^2 r^2 (\Delta S)}$$

(See Figure 1.) At the end of each interval, 10 mls of supernatant liquid were withdrawn and dried. The intervals used ranged from 20 -



(SVEDBERG and NICHOLS)

Figure 1. Method for Calculating Centrifuge Sedimentation Intervals



(HINCKLEY)

Figure 2. Computation of Crystallinity Index

Page missing from thesis

and less than 0.1 microns. Several methods have been proposed to analyze crystallinity, or stacking orderliness, using x-ray diffraction. The method used here was considered to be the most reliable. Random powder packs were prepared for each size fraction interval. X-ray diffraction patterns were generated for each and crystallinity index values were assigned according to the relationship presented in Figure 2.

Scanning and Transmission Electron Microscopy

Scanning electron microscopy (S.E.M.) and transmission electron microscopy (T.E.M.) were used to investigate both treated and non-treated samples. S.E.M. samples were sedimented onto aluminum stubs and coated with carbon and Au-Pd alloy. T.E.M. samples were suspended on a collodian film and were uncoated. Samples prepared for the microscopes were treated and dispersed in distilled water in order to reduce the possibility of contamination during preparation. S.E.M. was employed mainly to examine large aggregates produced through treatment with aluminum. The overall macroscopic morphology of the aggregates was evaluated in this manner. T.E.M. was used to analyze particle geometry and morphological features. Stereo-pair photographs were prepared on the T.E.M. for treated samples. The stereo pairs were instrumental in determining major particle alignment features.

Sodium Specific Ion Electrode

The cation exchange capacities of five size fractions were determined using a Corning NAS 11-18 sodium ion electrode. The procedure, as described by R. L. Malcolm et al. (1969), employs a sodium ion electrode rather than the traditional H^+ ion electrode for measuring

exchange capacities.

The clay fractions were washed five times in 1.0N NaCl. Approximately 1 gram samples were exchanged in this solution. Agitation, supplied by a Biosonic III ultrasonic unit, was used to assure total Na^+ exchange. Upon exchange completion, samples were washed with distilled water until no Cl^- could be detected. The standard AgNO_3 -chloride detection technique was utilized. Samples were dried at 110°C and 50 mg portions were weighed and separated. The 50 mg portions of Na^+ saturated kaolinite were added to beakers containing 10 mls distilled water. The suspensions were mixed, using the ultrasonic unit, for three minutes. The water-clay mixtures were poured rapidly into 50 ml portions of 0.2N BaCl_2 , adjusted to pH 9. Each sample was subjected to ultrasonic agitation for 2 minutes. Values of pNa for each sample were recorded using the sodium glass electrode and an Orion Research Digital pH meter, model 801. Meter calibration curves were generated using solutions with pNa values ranging from pNa 2-5. The pNa results obtained from each sample were referred to the calibration curve and used to calculate the amount of Na^+ replaced by Ba^{+2} . The general relationship used is as follows:

$$\text{C.E.C. (meq/100g)} = \frac{(\text{ppm Na}^+ \text{ at steady state} - \text{ppm Na}^+ \text{ at } t_0)(262.0)}{\text{mg of sample}}$$

Cation exchange capacities were determined for 2-1, 1-0.5, 0.5-0.25, 0.25-0.1 and 0.1-0 micron fractions.

Atomic Absorption Spectrophotometry

The amorphous Si-Al content of the kaolinite was identified and measured with a Perkin-Elmer Model 303 atomic absorption spectrophotometer. The sample preparation technique was described by Jackson (1969).

Approximately 1 gram of KS was washed repeatedly in a 5 percent KCl solution. Distilled water was used to remove soluble salts. A 0.1g portion of this sample was added to a solution of boiling 0.5N KOH. The suspension was boiled for an additional 2.5 minutes and quickly cooled in a water bath. The clay was separated from the supernatant liquid by supercentrifugation. The supernatant liquid was examined by atomic absorption to obtain a quantitative measure of amorphous Si-Al. Calibration curves were prepared using 0, 5, 10, 15 ppm solutions. Several attempts were made with the S.E.M. and T.E.M. to visually locate the amorphous coating. No satisfactory results were obtained.

Differential Thermal Analysis

A R. L. Stone D.T.A. System, model FS-2, was utilized to examine the possibility that changes in crystallinity might occur over the size range 2-0 microns. Size fractions, for which C.E.C. values were obtained, were also analyzed by D.T.A.

One hundred milligrams of KS, for each size fraction, were used for the analysis. The standard material used, Al_2O_3 , displays no phase change over the range of interest, 25-900°C. The sample and standard were loaded into their respective Inconel receptacles and heated to 900°C at a heating rate of 5°C per minute.

Enumerable theories have been proposed to explain the variations in D.T.A. traces of kaolinite. Murray (1956) suggests that various

trace features may be utilized to indicate the orderliness of internal structure. Each size fraction was evaluated and values for endothermic peak area, maximum peak temperature (T_{\max}), reaction initiation temperature (T_{start}), and return to base line temperature (T_{end}) were noted.

Characterization

X-ray diffraction analyses of KS indicate a relatively pure kaolinite containing only minor amounts of accessory minerals. The accessory minerals present include illite, quartz, rutile or anatase and talc. Characteristic XRD patterns are presented in Figure 3.

Crystallinity index values computed (Table 2) reveal either a decrease in stacking orderliness with decreasing size or simply a decrease in random orientation due solely to a fine-grained texture. D.T.A. analyses seem to confirm this crystallinity trend. Conclusions on the point will be drawn after reviewing D.T.A. results.

Scanning and transmission electron microscopy disclosed a kaolinite composed of few particles larger than 2 microns. Abundant fine particles (< 0.5 microns) dominate the field of view. Typical hexagonal platelets are noted (Figure 4).

Cation exchange values computed are very close to those expected. Grim (1968) reports cation exchange capacities which vary from 3 to 15 meq/100g clay. Table 3 records the C.E.C. values for each of the five size fractions. Exchange capacities increase with decreasing particle size due to an increased surface area (Grim 1968). This observation is consistent with data presented in this work.

Amorphous Si-Al is an integral part of most clay minerals.

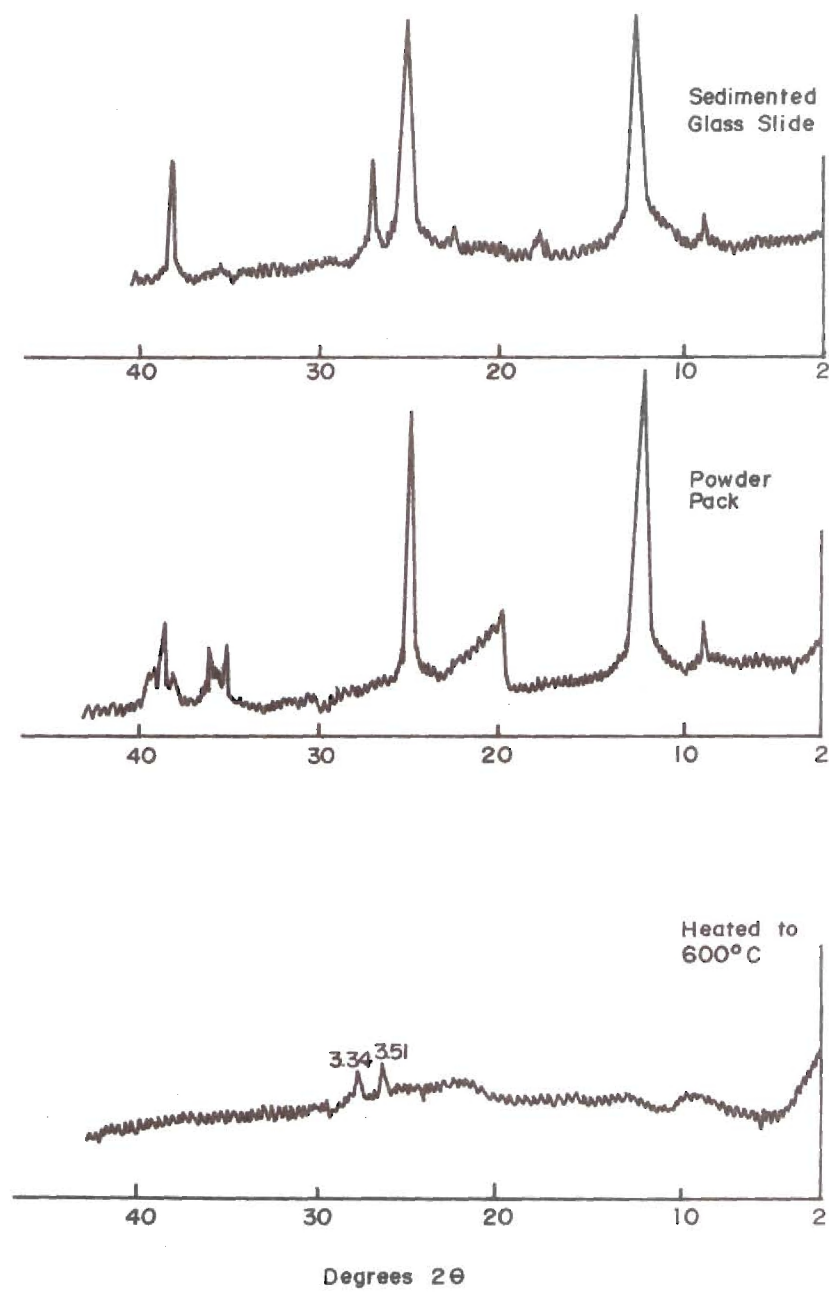


Figure 3. Diffraction Patterns for KS

Table 2. Crystallinity Index Values for KS

+ 1.0 micron	-	0.733
1.0 - 0.5 micron	-	0.525
0.5 - 0.25 micron	-	0.425
0.25 - 0.10 micron	-	0.412
0.10 - 0 micron	-	0.375

Table 3. Cation Exchange Capacities--KS

+ 1.0 micron	-	1.79 meq/100g
1.0 - 0.5 micron	-	3.80 meq/100g
0.5 - 0.25 micron	-	5.81 meq/100g
0.25 - 0.10 micron	-	6.16 meq/100g
0.10 - 0 micron	-	6.58 meq/100g

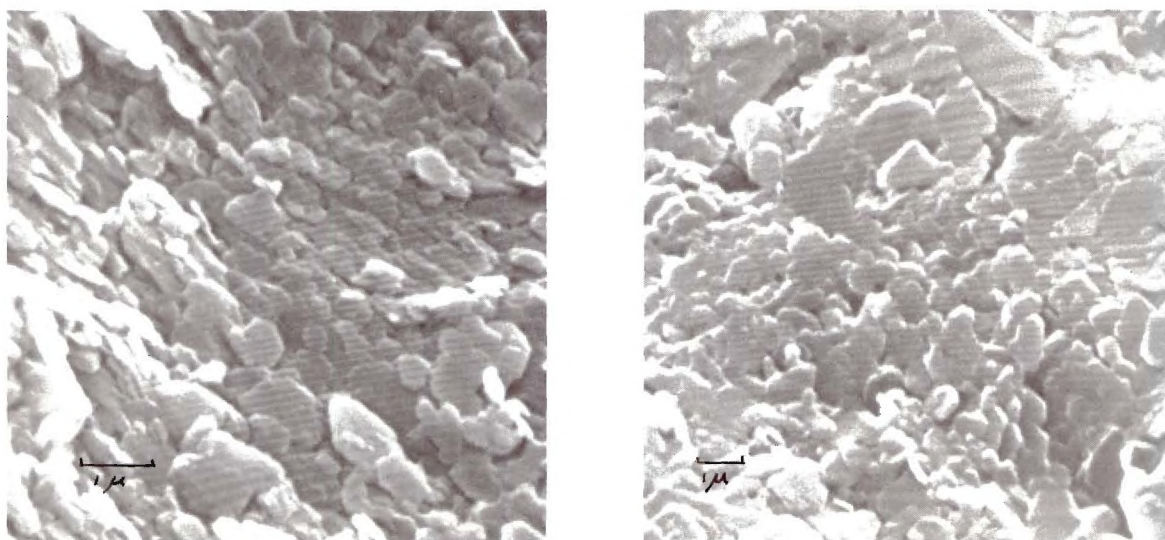


Figure 4a. S.E.M. Micrographs Illustrating Typical Fine-Grained Texture of KS

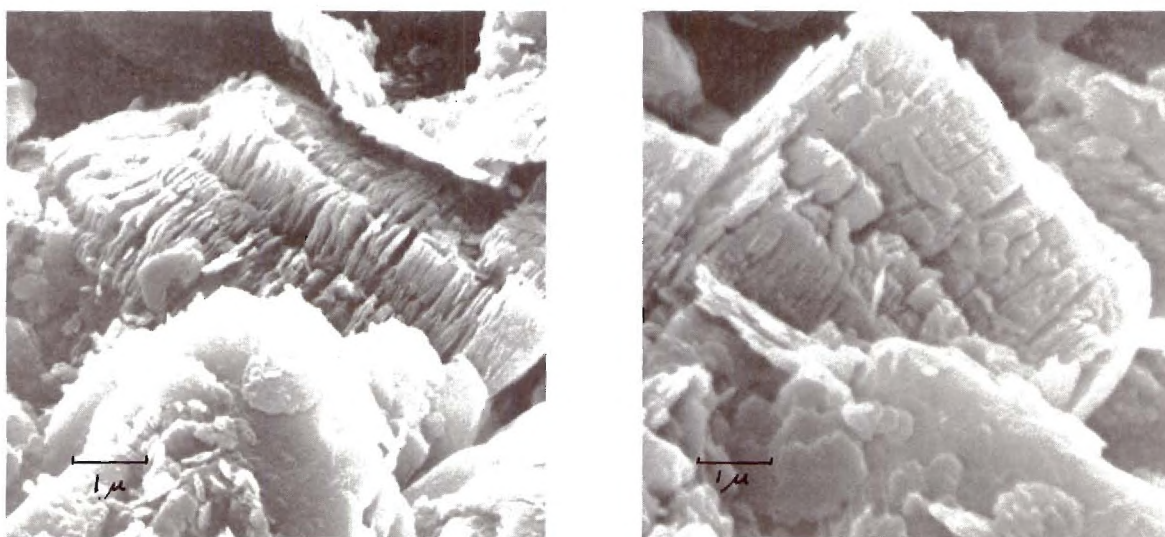


Figure 4b. Relatively Rare Large Kaolinite Books Found in KS

Occurring as a surface coating, it acts to inhibit true x-ray diffraction intensity. The material, though composed of definite elemental constituents, lacks sufficient internal order and therefore is difficult to identify using conventional x-ray diffraction. KS was found to contain approximately 3 percent total amorphous Si-Al. A large portion of this material may be adsorbed on the surface of an accessory clay mineral, illite. X-ray diffraction patterns of KS, both before and after treatment for amorphous material, exhibit a drastic change in illite peak intensity (Figure 5).

D.T.A. traces for five size fractions display a trend worthy of mention. Several authors such as Carthew (1955) and Grimshaw (1945) have concluded that the endothermic peak area for kaolinite remains constant regardless of particle size. Reaction initiation and completion temperatures are noted to vary, however, peak area reflects calories released and should only be affected by changes in sample quantity. Table 4 records a direct relationship between peak area and particle size. Having noted this fact, the possibility arises that, in this instance, internal orderliness might also increase with particle size. Larger peak areas infer more calories are needed in order to complete dehydroxylation. Highly crystalline material would be firmly bonded and more energy would be required to effect bond rupture. The trend in peak area is significant and represents a change other than particle size. The decrease in crystallinity with size, also noted on XRD, probably reflects the manner in which the smaller particles were produced, i.e., particle shear. The larger particles were subjected to weathering and smaller ones were produced which contained a

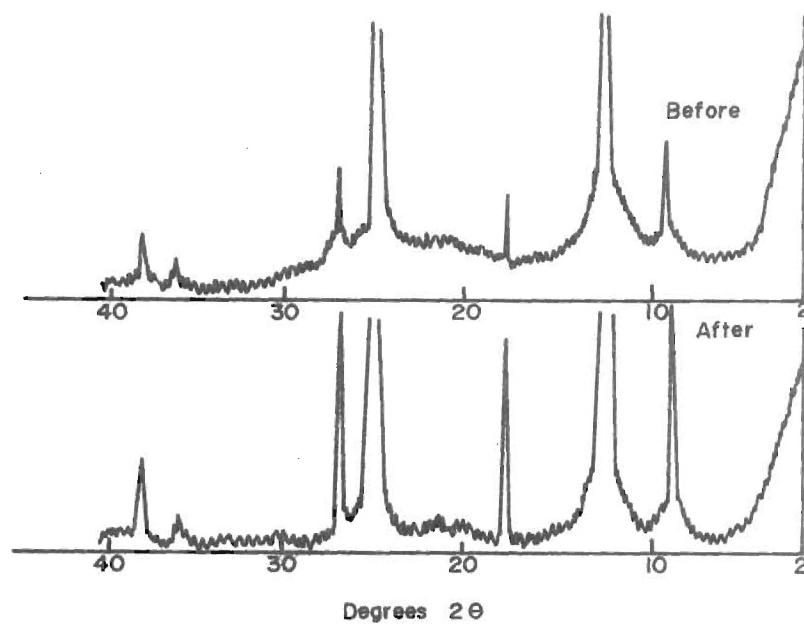


Figure 5. Effect of Amorphous Si-Al on Illite XRD Peak Intensity

Table 4. Effect of Particle Size on Dehydroxylation Peak Area, T_{\max} , T_{start} , and T_{end}

Particle Size	Area	T_{\max}	T_{end}	T_{start}
1-2 microns	2.85 in. ²	536°C	600°C	400°C
0.5-1	2.76	532	576	402
0.25-0.5	2.73	529	586	401
0.1-0.25	2.67	531	579	383
0-0.1	2.64	527	563	385

characteristic amount of internal strain proportional to the intensity of weathering. The strain manifests itself as a change in crystallinity.

A complete size analysis of the kaolinite sample, contrasted with a kaolinite of higher coating quality (KB), is seen in Figure 6. The two distribution curves show marked differences especially at particle sizes below 2 microns. The variation between curves in this region (2-0 microns) serves to exemplify the drastic differences in coating properties. The percentage finer than 0.5 microns was chosen as a reference value and all treated samples were examined at this point. Values obtained were compared to the untreated standard value. Any deviations from this standard value indicate a change in the size distribution. Values lower than the standard are considered positive and indicate particle aggregation.

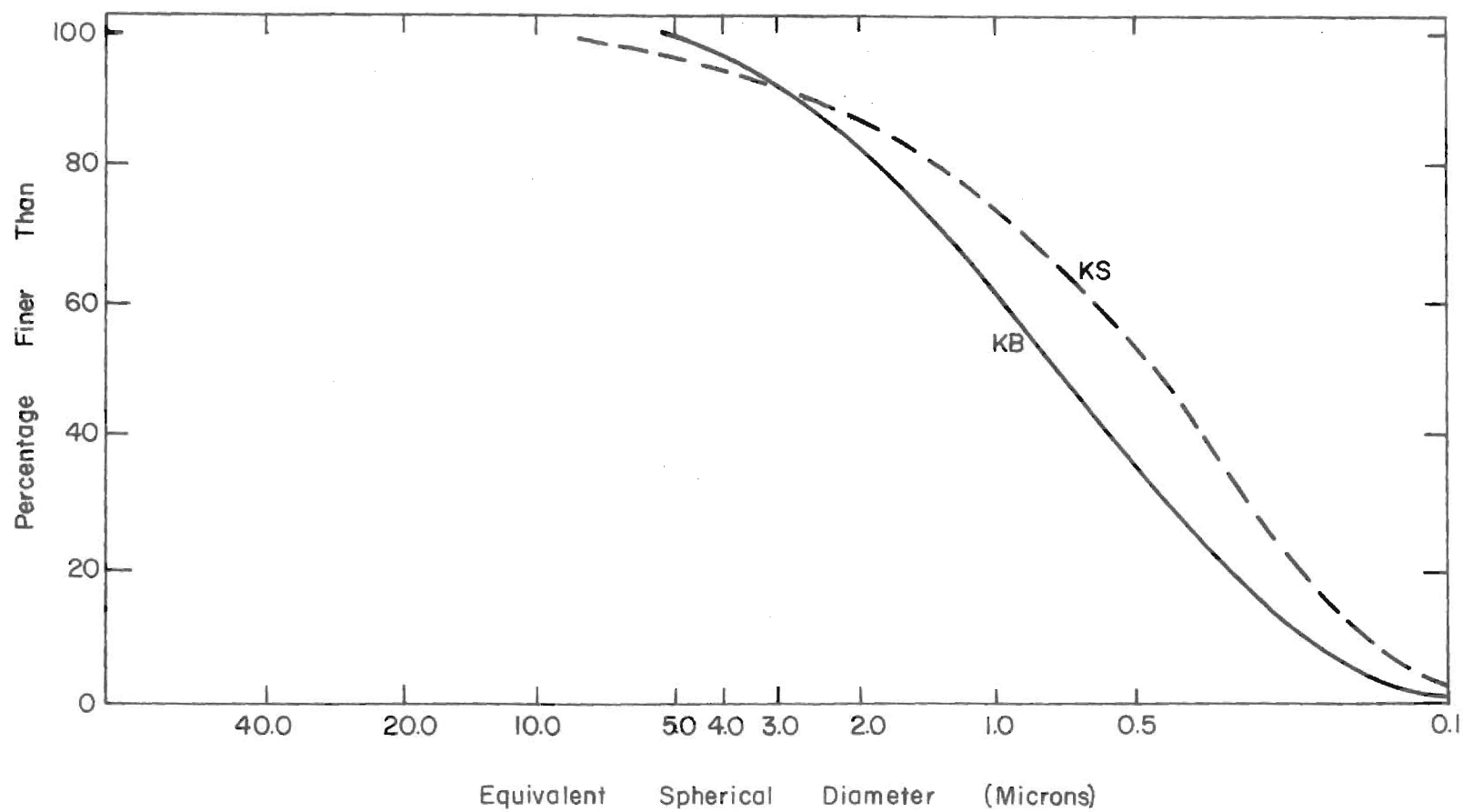


Figure 6. Particle Size Distribution for KB, KS

CHAPTER III

ALUMINUM TREATED KAOLINITE

Treatment

Several 1 gram samples of KS were placed in an oven at 110°C to remove adsorbed water. The samples were then evaluated at 0.5 microns to determine if simple drying could effect particle size changes. Other samples were subjected to five wet-dry cycles and then examined. No significant particle size alteration was recorded for any sample. Simple drying was eliminated as a source of clay-clay bonding. Before 1 gram treated samples were evaluated at 0.5 microns, they were blended for five minutes using 5 mls of 4g/l sodium polyphosphate as a dispersant. The technique not only supplied agitation necessary for complete dispersion but also introduced a standard amount of shearing energy. Cemented aggregates should not dissociate during the process. It is necessary that the samples withstand these forces because they are representative of normal plant processes.

The original clay-hydroxy aluminum interaction hypothesis was analyzed by preparing solutions of AlCl_3 and NaOH . Ratios of OH/Al in prepared solutions ranged from 0.1-3.0. Aluminum was held constant at 0.02 m/l. The solutions were prepared by adding 0.1N NaOH dropwise to 10 mls 0.2N AlCl_3 and a predetermined portion of distilled water. The distilled water was added to insure each final mixture would contain 100 mls of solution. One gram samples, sieved less than 44 microns,

were added to each solution. Two minutes of agitation was supplied by the ultrasonic mixer. All treated samples were dried at 150°C . The percentage finer than 0.5 microns was computed and plotted versus OH/Al ratio. The resulting curve, Figure 7, displays a saw tooth type configuration. Percentages recorded lie far below those for untreated clay. Particles greater than 44 microns were noted. Particle aggregation had apparently occurred during the process. Clay minerals possess the ability to remove ions from solution (Grim 1968). For this reason, a series of samples were aluminum exchanged with 0.1N AlCl_3 prior to treatment with aluminum solutions. The exchange treatment would theoretically allow all exchange positions to become occupied with aluminum. As aluminum solutions are added to exchanged samples, no aluminum would be removed from the suspension. The law of mass action would provide no driving force for exchange and therefore all aluminum introduced to the system would be available for cementation. Table 5 records observed percentages less than 0.5 microns for samples treated with OH/Al ratios = 0.1. Once the relationship involving aluminum exchange was established, no further samples were pre-treated in this manner. It should be noted, however, that aluminum exchanging does slightly amplify cementation.

The economic feasibility of cementation must be considered. Six solutions of AlCl_3 and NaOH (OH/Al = 0.5) were prepared with various proportions of chemicals ranging from 0.3-12.0 weight percent. The experiment allows estimation of chemicals needed to effectively alter the particle size distribution for 1 gram samples of KS. Table 6 records proportions of chemicals used in the experiment. One gram samples of KS were added to each 100 ml solution and agitated for three minutes.

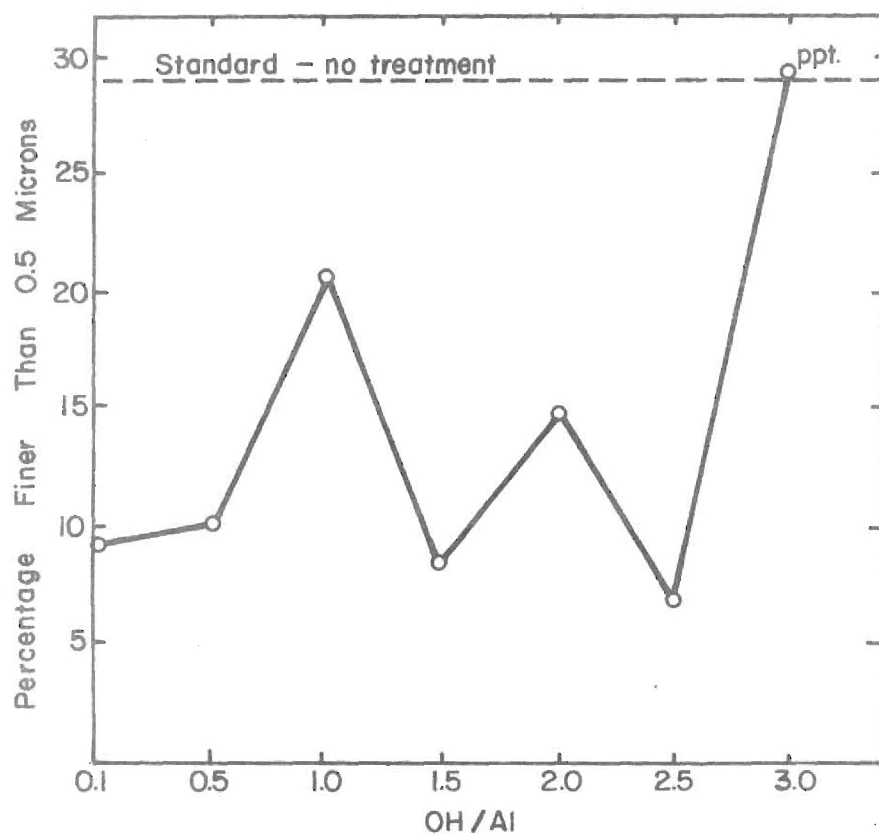


Figure 7. Effect of OH/Al Ratio on Cementation

Table 5. Changes in Cementation Resulting from Aluminum Exchange Prior to Treatment with AlCl_3

Sample	#1	#2	#3
KS Standard - No treat.	28.5*	27.2*	27.5*
KS - Treated	13.8*	14.6*	14.2*
KS - Al. Exchanged-treat.	10.5*	11.1*	12.2*

* Percentage finer than 0.5 microns.

Table 6. Alterations in Cementation with Increasing Weight Percent Chemicals Added

Wgt. Percent	AlCl_3 (0.002M)	NaOH (0.001M)	Percentage finer than 0.5 microns
0.3	10 ml	10 ml	32.06
0.6	20	20	33.90
1.2	40	40	30.48
	AlCl_3 (0.02M)	NaOH (0.01M)	
3.0	10	10	26.39
6.0	20	20	24.52
12.0	40	40	18.30

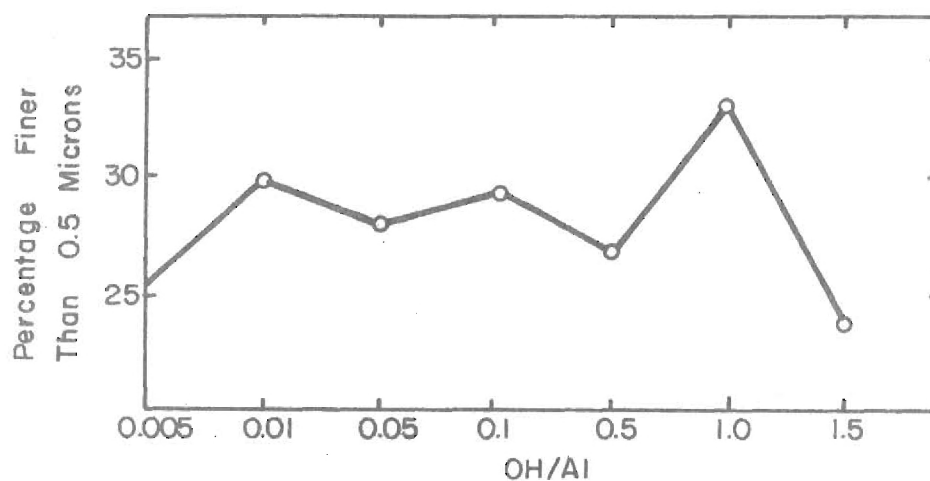


Figure 8. Cementation Over a Range of OH/Al Ratios From 0.005-1.5

Percentages finer than 0.5 microns were computed as described previously.

The OH/Al ratio in aluminum solutions controls the magnitude of the positive charge displayed by the aluminum complexes. Smaller ratios produce more highly charged species. Hydroxy-aluminum solutions were prepared with OH/Al ranging from 0.005-1.5. Aluminum was constant at 0.002 m/l. One hundred milliliters of solutions were used to treat 1 gram samples. No significant change in cementation was noted over the entire range (Figure 8). The small amount of NaOH present at OH/Al = 0.005 indicates a lesser dependence on externally added OH^- . From this data, it appears that sufficient complexes may be created in stock AlCl_3 solutions to cement 1 gram of kaolinite. Hydroxide, added as NaOH, provides an abundance of anions which serve to reduce the effective positive charge exhibited by aluminum complexes. In order to evaluate this hypothesis, several 1 gram samples of KS were treated with solutions of AlCl_3 . One hundred milliliters of AlCl_3 was added to 1g samples of KS. Mixtures were agitated for three minutes. Samples were dried at 150°C . Dried samples were subjected to the standard amount of shear as previously described. The AlCl_3 solutions produced cemented aggregates which were comparable to those noted using NaOH as a source of OH^- . Solutions of AlCl_3 were prepared, in varying concentrations, using distilled water at pH 6. Resulting solutions displayed drastic reductions in pH. Solutions more concentrated in aluminum exhibited lower pH values. The change in pH during solution preparation was due to the hydrolysis of aluminum. The H^+ ion concentration increases as OH^- is coordinated about the Al^{+3} . It appears evident that the amount of aluminum complexes formed in stock solutions is sufficient to cement 1 gram samples of KS.

One hundred milliliter portions of AlCl_3 solutions were prepared with total aluminum ranging from 10^{-6} - 10^{-1} moles. The solutions were prepared by effecting the appropriate dilutions of a 1.0N AlCl_3 solution. Solutions were agitated, as described previously, and one gram portions of KS were added. Samples were dried at 150°C . The resulting curve (Figure 9) illustrates both the amount of aluminum necessary for cementation and the maximum particle alteration possible using AlCl_3 solutions. Six separate, identical experiments of this type were conducted to insure the validity of the curve. The curve will be referred to as the "working curve." A working relationship between degree of cementation and total moles aluminum in solution was established. Having established the above relationship, other influential factors in the cementation mechanism were analyzed. Figure 10 records results obtained by the alteration of solution pH. One gram samples of KS were added to 10 beakers containing 100 mls of 2×10^{-2} m/l AlCl_3 . The solutions were thoroughly mixed. Two samples were adjusted to each major pH unit between pH 3 and 7. Adjustments were accomplished with 0.1N NaOH and 0.1N HCl. Two samples were assigned to each pH unit in order to validate results. Samples were dried at 150°C and, using the standardized procedure, deviations from a standard at 0.5 microns were calculated.

An experiment was established to examine the relationship between cementation and aluminum concentration. A relationship was previously established between cementation and total moles aluminum. Table 7 records various concentrations of treating solutions. One gram samples were treated with each solution and evaluated at 0.5 microns (Figure 11). Though the molarity (m/l) of aluminum varied over a wide range

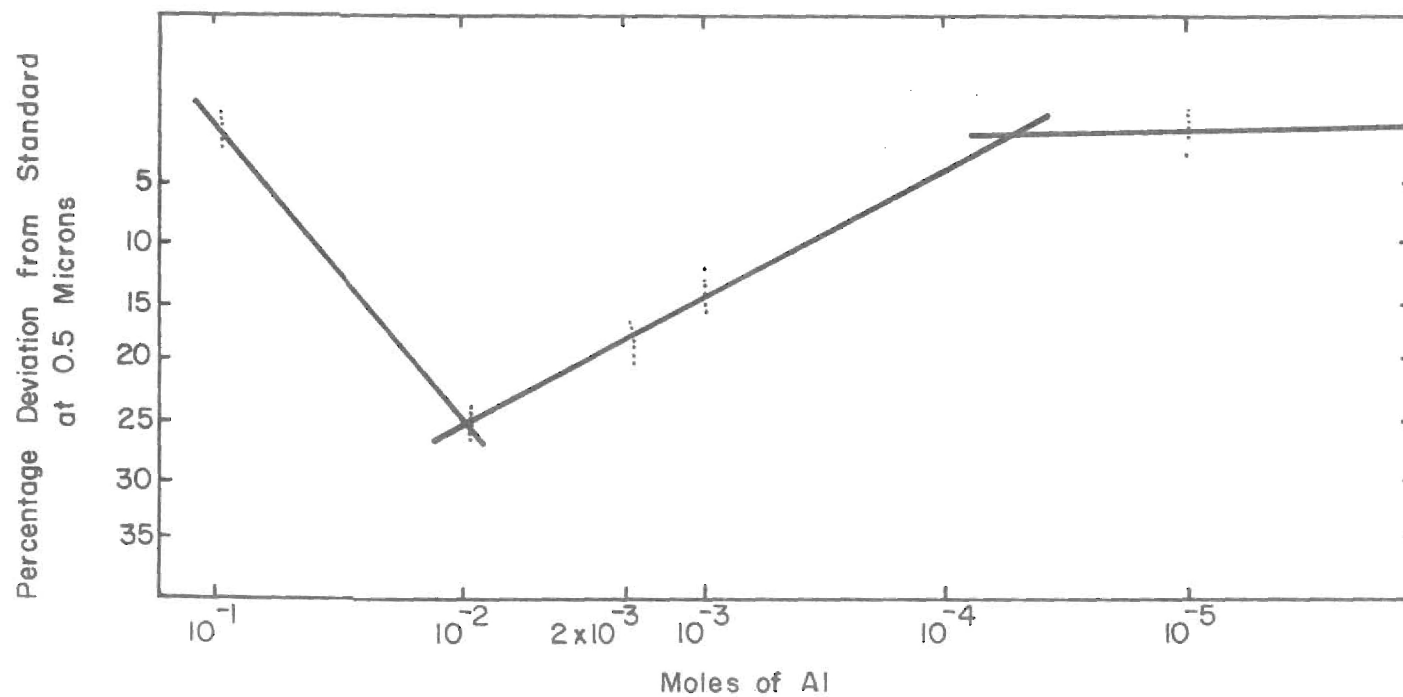


Figure 9. Range of Cementation Using 1 Gram KS and AlCl_3

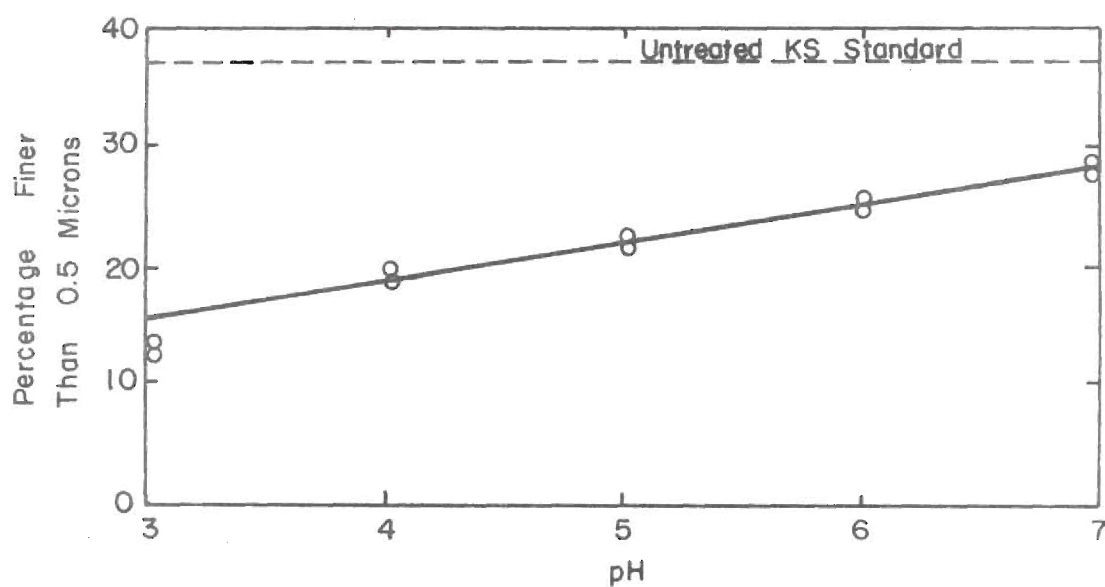


Figure 10. The Effect of pH on Cementation

Table 7. Concentrations of AlCl_3 Used to Evaluate Cementation

Treatment Solution			
25 mls	50 mls	100 mls (working curve)	Total Al
$8 \times 10^{-2} \text{ m/l}$	$4 \times 10^{-2} \text{ m/l}$	$2 \times 10^{-2} \text{ m/l}$	$2 \times 10^{-3} \text{ moles}$
4×10^{-2}	2×10^{-2}	10^{-2}	10^{-3}
4×10^{-3}	2×10^{-3}	10^{-3}	10^{-4}
4×10^{-4}	2×10^{-4}	10^{-4}	10^{-5}
4×10^{-5}	2×10^{-5}	10^{-5}	10^{-6}

(8×10^{-2} m/l - 10^{-5} m/l), the curves generated are identical with the working curve. The only common factor is total moles aluminum. It seems apparent that the molarity of the treating solution is secondary when compared to total moles of aluminum present.

Simple drying of samples (untreated) at 110°C had previously proven to be ineffectual at cementation. Treated samples, however, display marked fluctuations in cementation as the temperature of drying is varied. Aluminum chloride solutions were prepared to evaluate changes in cementation, for each 50°C interval, over a temperature range of $50 - 300^{\circ}\text{C}$. For each interval, AlCl_3 solutions were prepared containing 10^{-6} , 10^{-4} and 2×10^{-3} moles aluminum. The samples corresponded to 100 milliliters each of 2×10^{-2} m/l, 10^{-3} m/l and 10^{-5} m/l AlCl_3 . Samples were heated at their respective temperatures until dry. Evaluation at 0.5 microns produced results as seen in Figure 12. The sample dried at 50°C could not be dispersed with standard treatment. In view of changes of cementation with treated samples, it became necessary to examine untreated samples over a range of temperatures. Standard untreated samples of KS (lg) were dried, from 100 mls of distilled water, at temperatures ranging from $50 - 400^{\circ}\text{C}$. Each 50°C increment was analyzed. The resulting curve (Figure 13) reveals a deviation from the typical value for KS, at 250°C . At temperatures greater than 250°C , the percentage finer than 0.5 microns is drastically altered.

Solutions of $\text{Al}(\text{NO}_3)_3$ and $\text{Al}_2(\text{SO}_4)_3$ were also used to treat KS. Five solutions of aluminum nitrate were prepared comparable in aluminum content to the series prepared for the working curve evaluation. The experiment was duplicated using aluminum sulfate as a source of aluminum.

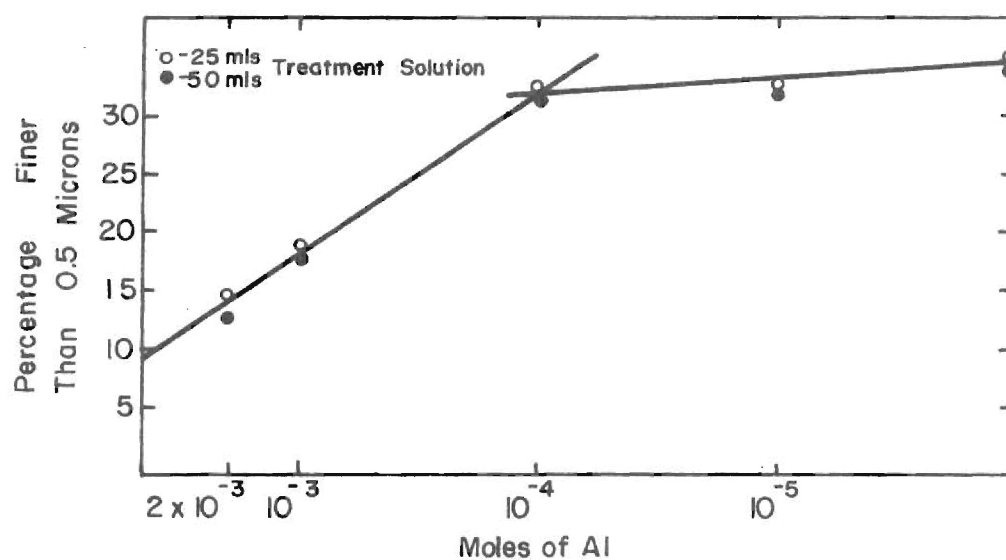


Figure 11. The Effect of Treatment Solution Concentration on Cementation

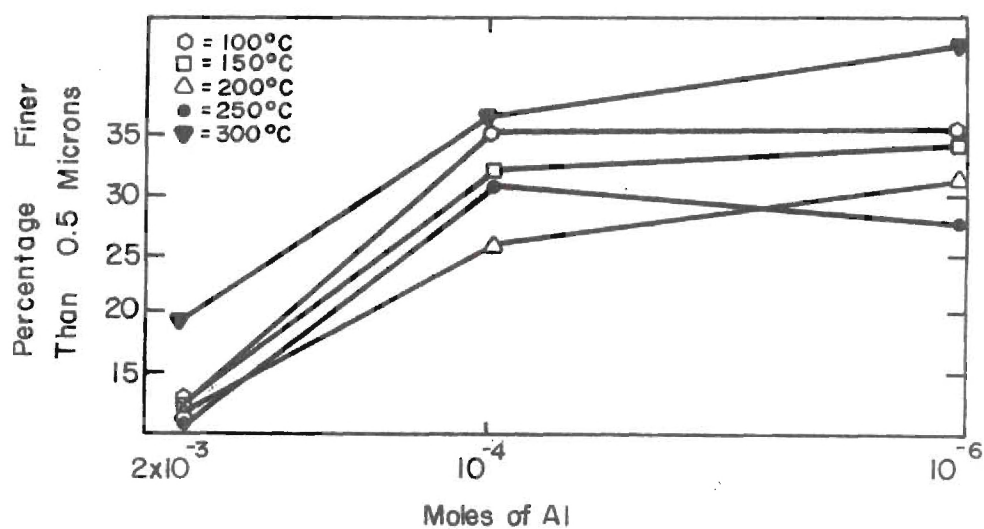


Figure 12. Cementation as a Function of Drying Temperature

The samples were dried at 150°C and examined at 0.5 microns. Both sets of solutions remained flocculated, even after attempted dispersion. No accurate data could be obtained concerning possible cementation.

Results and Discussion

Drastic alterations in the size distribution for aluminum treated KS reflects a definite cementation mechanism. A complete size distribution for 1 gram of KS, treated with 100 mls 2×10^{-2} m/l AlCl_3 , is contrasted with its untreated counterpart in Figure 14. The cementation responsible for the disparity in distribution curves is dependent on several factors. The four deemed the most important were examined. Other factors, such as ageing, were not considered to be of primary interest and were not evaluated.

Total Moles Aluminum

It is apparent when examining the "working curve" (Figure 9) that cementing, once initiated, increases with moles aluminum added. Figure 11 elucidates the dependence on total moles of aluminum in the treatment solutions. Aluminum was added to 1 gram samples of KS in varying concentrations. Even though the concentration and amount of treating solution varied, the resulting curve is identical to the "working curve." Total moles aluminum is the only factor common to both curves. A change in slope is noted at approximately 5×10^{-5} moles aluminum. The same break in slope occurs in the "working curve" and indicates the initiation of cementation. It is believed that the ability of kaolinite to remove ions from solution is responsible for the concentration dependence noted. The equivalents of aluminum necessary for initial cementation corresponds

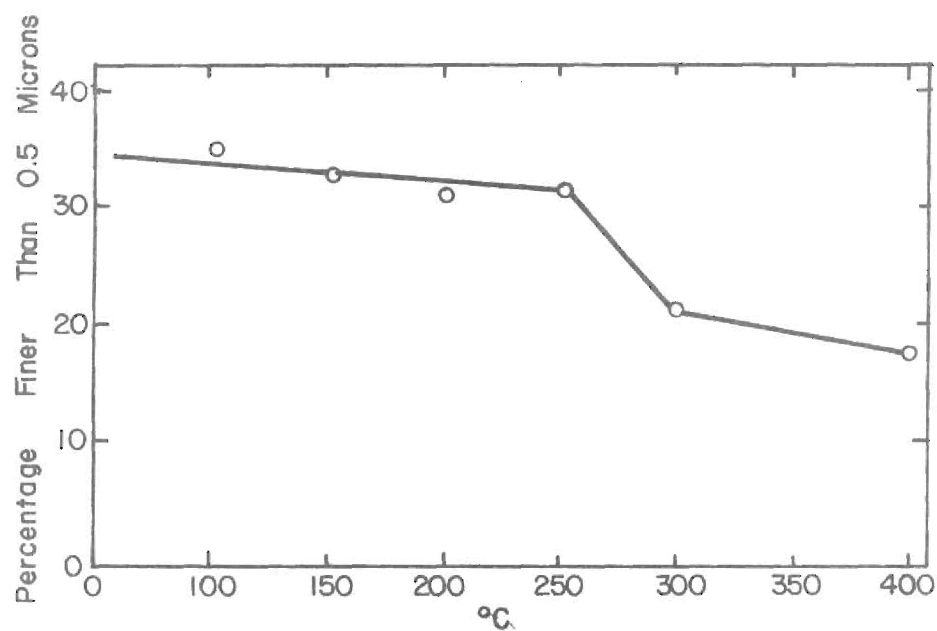


Figure 13. Particle Size Alteration of Untreated Standards Over a Range of Drying Temperatures

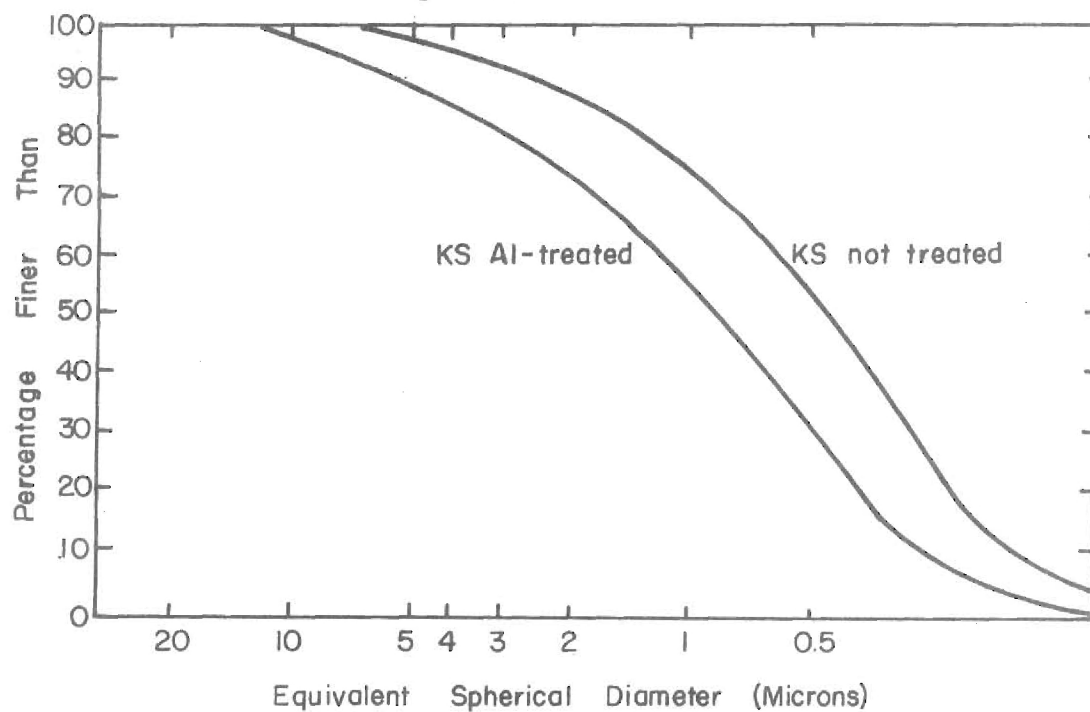


Figure 14. Particle Size Distribution for Treated and Untreated KS

to a C.E.C. of 5 meq/100g KS. Exchange capacities reported in this work range from ~2-7 meq/100g. It is theorized that until the exchange sites have satisfied their demand for Al^{+3} , no aluminum will be available for cementation. Several samples were aluminum exchanged prior to treatment in order to examine possible deviations from the "working curve." Noted differences were slight and actual gains in cementing efficiency were not separable from those which may have been produced through experimental error.

Al^{+3}

Although initially formed aluminum complexes were thought to effect cementation, aggregation appears to increase with Al^{+3} concentration. Figure 15, plotted from results reported by Parks (1972), illustrates the distribution of the various species of aluminum present over a range of pH values. With the aid of Figure 15, Figure 16 was generated. The figure indicates that cementation is initiated only after the abundance of Al^{+3} has exceeded total existing aluminum complexes. The absolute effects of total aluminum and Al^{+3} are difficult to separate since Al^{+3} increases with total aluminum. In order to examine the influence of Al^{+3} , several solutions of 2×10^{-2} m/l $AlCl_3$ were prepared at pH values between 3 and 7. One gram samples were treated with 100 ml portions of the solutions. The resulting curve, Figure 10, reflects the absolute dependence on Al^{+3} . The only factor varying with pH is total Al^{+3} . Free aluminum is essential for the initiation of effective cementation.

Temperature of Drying

Examining the results of heating (Figure 12) it becomes apparent

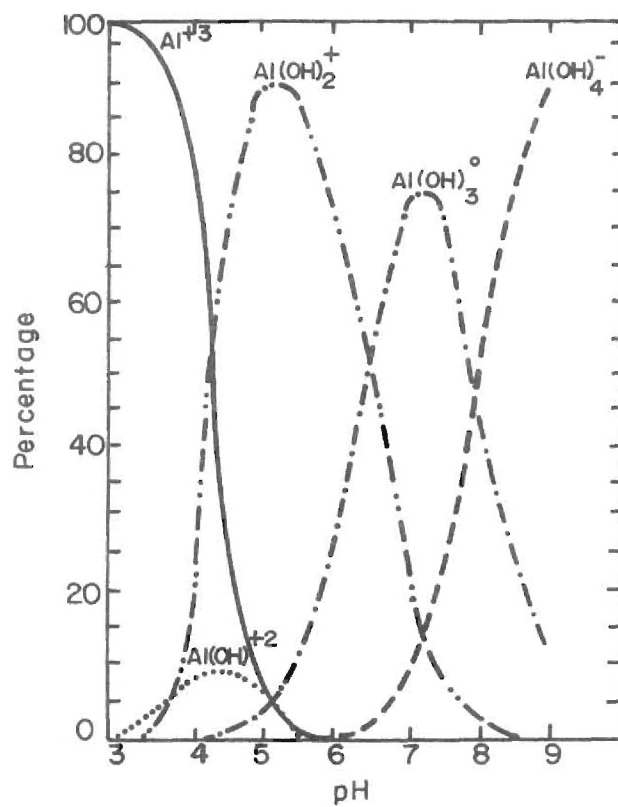


Figure 15. The Distribution of Aluminum Species in Aqueous Solution

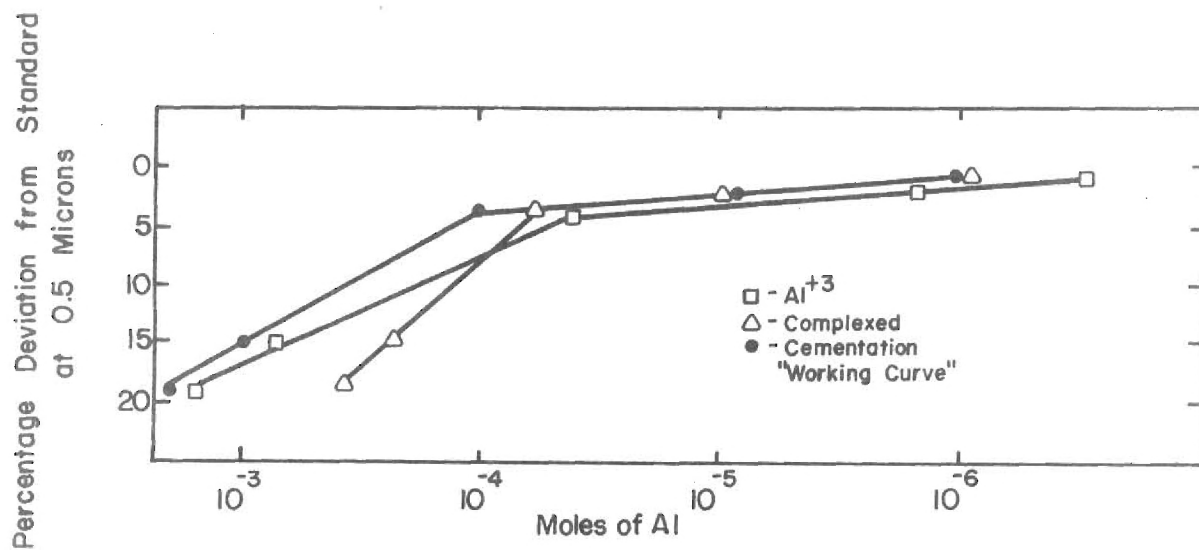


Figure 16. The Abundance of Complexed and Free Al^{+3} Related to Cementation

that the temperature of drying, for treated samples, assumes an important role in aggregation. C. I. Rich (1960) reported findings which indicate an increase in the polymerization of AlCl_3 with elevated temperatures. Turner (1967) also concluded that the stability of aluminum polymeric ions is enhanced by higher temperature. Conclusions of this nature, and experimental data, indicate that the actual cementing agent is probably newly complexed aluminum polymers, created as a result of heating, or existing polymers experiencing an elevated positive charge due to anion removal. A high concentration of Al^{+3} is necessary to form new polymers upon drying. It is these units which probably act to bind particles together.

Treated samples dried at temperatures above 200°C reflect a decrease in cementing effectiveness. The drastic reversal occurs at approximately 250°C . Untreated samples, however, exhibit a sharp increase in aggregation near the same temperature. It is believed that temperatures greater than 250°C serve to activate the amorphous Si-Al present. Untreated samples use this material as a cement while the addition of AlCl_3 deactivates the cementing mechanism. The formation of an amorphous precipitate is likely. The creation of a new stable phase serves to deactivate available aluminum.

Anions

Three aluminum compounds were evaluated as to their cementing effectiveness; AlCl_3 , $\text{Al}(\text{NO}_3)_3$ and $\text{Al}_2(\text{SO}_4)_3$. The resulting data indicate that the nature of anion present also exerts an influence over cementation. All samples treated with $\text{Al}_2(\text{SO}_4)_3$ were hopelessly flocculated even after drying and the addition of polyphosphate. Samples

dried with $\text{Al}(\text{NO}_3)_3$ remained slightly flocculated. The samples were impossible to examine quantitatively, using standardized techniques, due to their flocculated state. It was noted, however, that no cemented particles > 44 microns were present with $\text{Al}_2(\text{SO}_4)_3$ and only a few with $\text{Al}(\text{NO}_3)_3$. Abundant particles of this size are produced with AlCl_3 .

Bundy and Murray (1973) reported findings concerning the flocculation characteristics of kaolinite in the presence of $\text{Al}_2(\text{SO}_4)_3$. Their findings indicate that where $\text{SO}_4^{=}$ is relatively concentrated, edge-edge and edge-face structures dominate. As sulfate was selectively removed from the system, they noted that face-face association increased. It was theorized by the investigators that positively charged aluminum hydroxide, relatively free of sulfate, aggregates on the clay surface. Maximum decreases in surface area were noted for this situation.

The removal of anions is an essential step in aggregation. Increased temperatures ($> 100^\circ\text{C}$) serve to rid the solution of Cl^- whereas $\text{SO}_4^{=}$ is rather stable and difficult to remove by this process. An AlCl_3 treated sample, which was described earlier, was dried at 50°C . The sample could not be dispersed and therefore was impossible to evaluate. No cementation was evident. The depressed drying temperature allowed the water to be removed while concentrating Cl^- . The effect of concentration was to reduce the possibility that any unsatisfied charges would be available from aluminum complexes. The abundant available chloride served to satisfy all existing charge unbalances and thus no clay-aluminum hydroxide complexes were formed. Bailar (1956) introduced the term "anion penetration" to represent the tenacity with which anions bond to aluminum complexes. He proposed a "penetrating power" hierarchy

in which $\text{Cl}^- < \text{NO}_3^- \ll \text{SO}_4^{=}$. Anions serve to satisfy any existing positive charges on aluminum complexes. In this manner a neutral species is produced which is not responsive to the clay present. It is necessary, therefore, to remove anions and allow face-face association to increase. Cementation of face-face aggregates represents the most efficient method of reducing the surface area.

Stereo T.E.M. micrographs allow morphological evaluation of cemented flakes. Aggregates appear to be composed of small particles aligned along the "C" axis of larger flakes (Figure 17). S.E.M. and T.E.M. micrographs are also reproduced to assist in examining cemented aggregates (Figure 18).

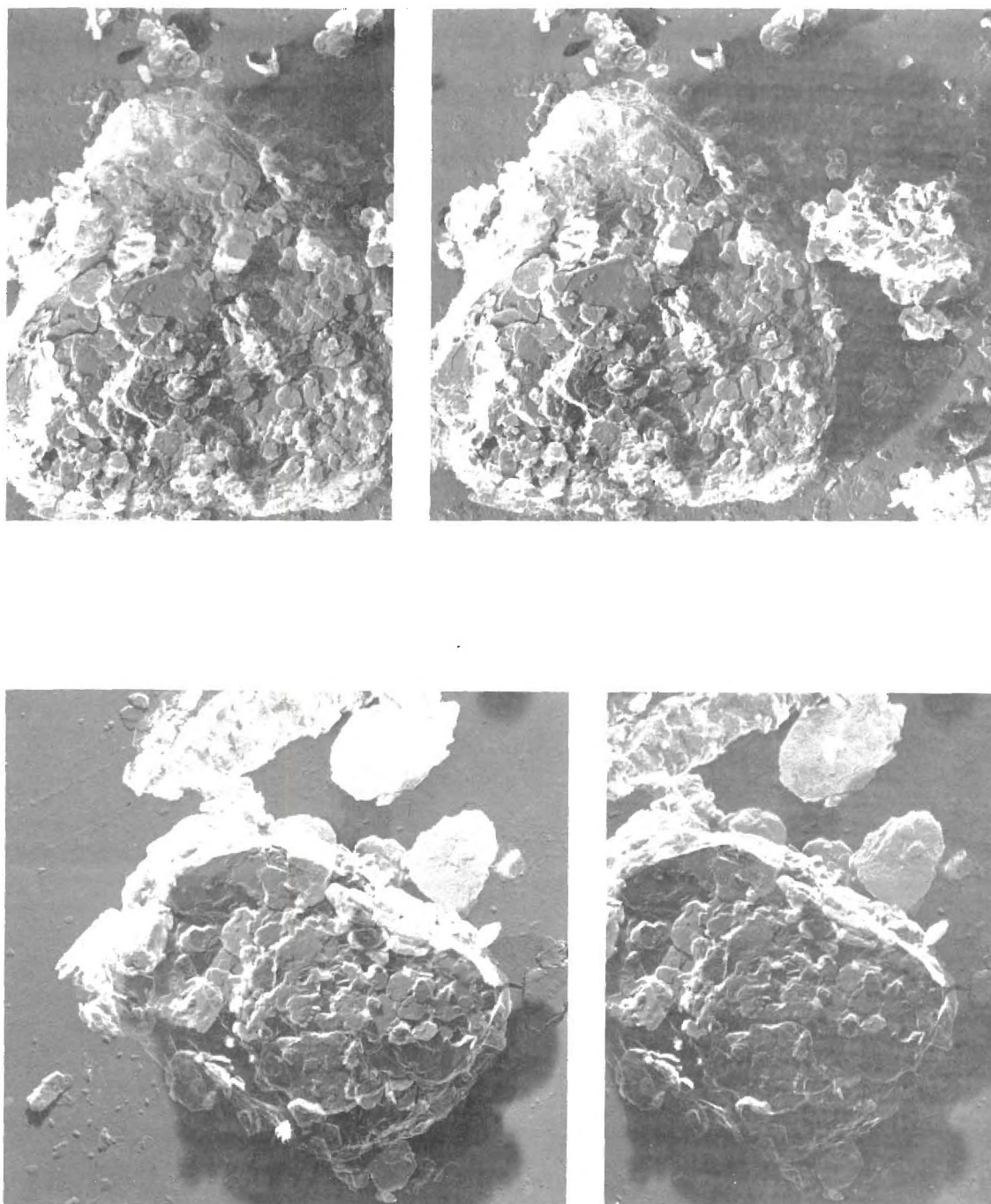


Figure 17. Stereo T.E.M. Micrographs Revealing Morphology of Cemented Kaolinite

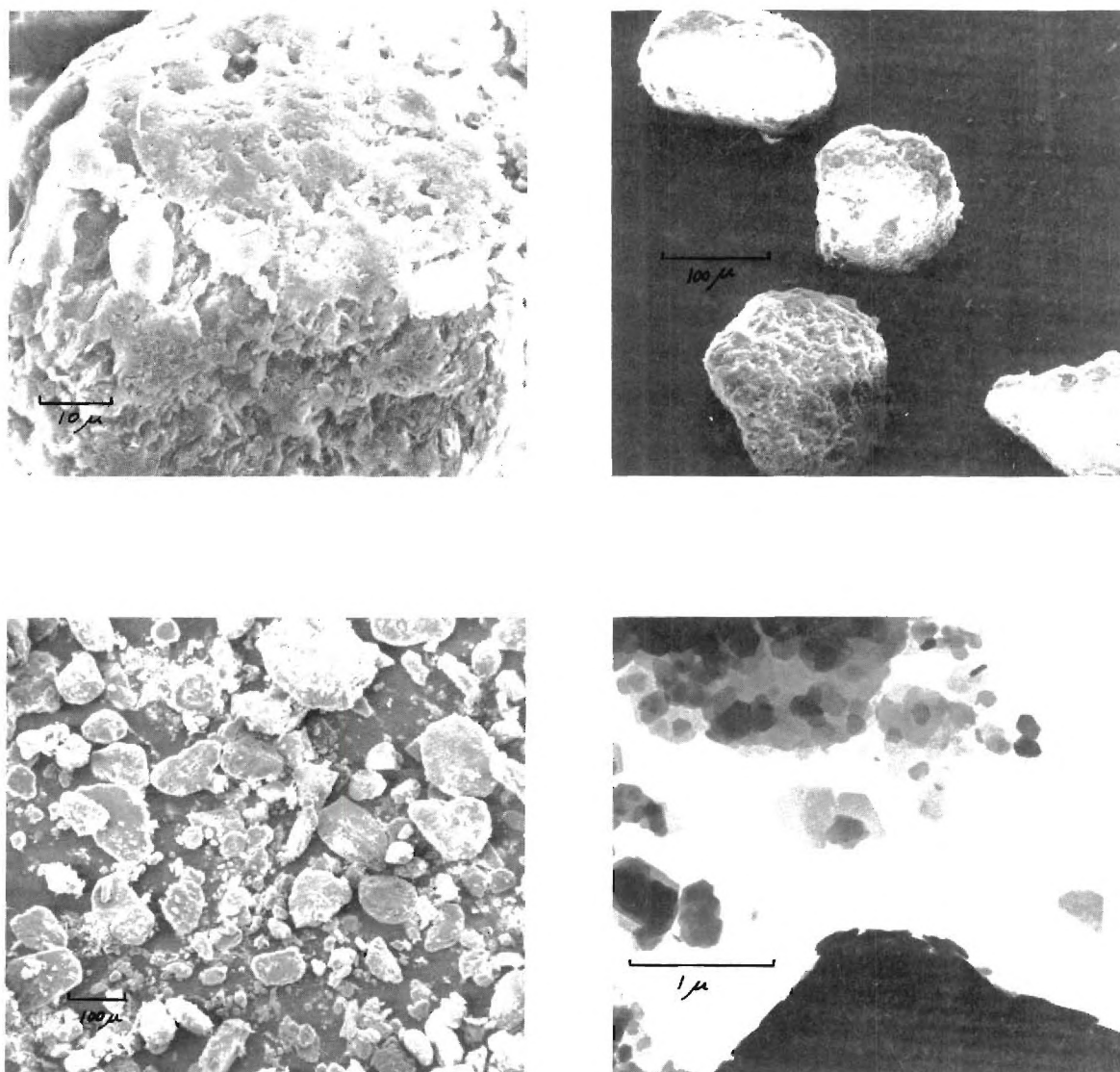


Figure 18. S.E.M., T.E.M. Micrographs of Cemented Kaolinite Particles (Rounded Edges are Due to Attempted Blender Dispersion)

CHAPTER IV

CONCLUSIONS

Aluminum can be utilized as an effective agent for the cementation of kaolinite flakes. Although several factors exhibit influence over the degree of cementation, reproducible results can be obtained through careful examination of these factors.

The economic feasibility of commercially using aluminum for aggregation may be questionable, however, certain basic information on kaolinite has been established.

Basic techniques and methods of examination have been proposed and will make possible the analysis of similar cations. Forms of hydroxide such as iron and magnesium may also be effective as a cementation agent.

Evaluation of the results and conclusions presented in this work may be of significance in interpreting factors necessary for the formation of aluminum hydroxide minerals such as gibbsite. Examination may also give insight into the environmental conditions necessary for the growth and stability of certain clay minerals.

BIBLIOGRAPHY

1. Bailar, J. C. (1956), The Chemistry of the Coordination Compounds, Reinhold Pub. Corp., New York.
2. Bundy, M. and H. H. Murray (1973), The Effect of Aluminum on the Surface Properties of Kaolinite, Clays and Clay Minerals, 21, 295-302.
3. Carthew, A. R. (1955), The Quantitative Estimation of Kaolinite by Differential Thermal Analysis, American Mineralogist, 40, No. 107.
4. Follett, E. A. C. (1965), The Retention of Amorphous, Colloidal Ferric Hydroxide by Kaolinite, Journal of Soil Science, 16, 334.
5. Grim, R. E. (1968), Clay Mineralogy, McGraw-Hill Book Company, New York.
6. Grimshaw, R. W., E. Heaton and A. L. Roberts (1945), Constitution of Refractory Clays, II, Thermal Analysis Methods, Trans. British Ceramic Society, 44, No. 76.
7. Hinckley, D. N. (1961), Mineralogical and Chemical Variations in the Kaolin Deposits of the Coastal Plain of Georgia and South Carolina, Penn. State Univ. NSF Tech. Report.
8. Hsu, P. and T. F. Bates (1964), Formation of X-Ray Amorphous and Crystalline Aluminum Hydroxides, Mineralogical Magazine, London, 33, No. 264, 749-768.
9. Jackson, M. L. (1956), Soil Chemical Analysis - Advanced Course, Published by the author, Dept. of Soil Science, University of Wisconsin, Madison, Wisconsin 53706.
10. Jackson, M. L. (1963), Aluminum Bonding in Soils: A Unifying Principle in Soil Science. Soil Science Society of America Proceedings, 27, No. 1.
11. Jenny, H. and Guy D. Smith (1935), Colloidal Chemical Aspects of Clay Pan Formation in Soil Profiles, Soil Science, 39, 377-89.
12. Malcolm, R. L. (1969), Determination of Cation Exchange Capacity with the Potassium Specific-Ion Electrode, Proceedings of the International Clay Conference, Tokyo, 1, 573.
13. Murray, H. and S. C. Lyons (1956), Correlation of Paper-Coating Quality with Degree of Crystal Perfection of Kaolinite, Clays and

Clay Minerals 14th Nat. Conf. Acad. Sc . NRC Pub. 456, 31-40.

14. Parks, G. A. (1972), Free Energies of Formation and Aqueous Solubilities of Aluminum Hydroxides and Oxide Hydroxides at 25°C. American Mineralogist, 57, 1163.
15. Rich, C. I. (1960), Aluminum in Interlayers of Vermiculite, Soil Science Society of America Proceedings, 24, 26-32.
16. Svedberg, T. and J. B. Nichols (1923), Determination of Size and Distribution of Size of Particle by Centrifugal Methods, Journal Amer. Chem. Society, 45, 2910.
17. Turner, R. C. (1967), Aluminum Removed from Solution by Montmorillonite, Canadian Journal of Soil Science, 47, 217.